VIROLOGICA SINICA

Electronic Supplementary Material

Structure and Function of N-Terminal Zinc Finger Domain of SARS-CoV-2 NSP2

Jun Ma[1], Yiyun Chen[2], Wei Wu[1], Zhongzhou Chen[1]✉

[1]State Key Laboratory of Agrobiotechnology and Beijing Advanced Innovation Center for Food Nutrition and Human Health, College of Biological Sciences, China Agricultural University, Beijing100193, China
[2]Cherry Creek High School, 9300 East Union Avenue, Greenwood Village, CO 80111, USA

Supporting information to DOI: 10.1007/s12250-021-00431-6

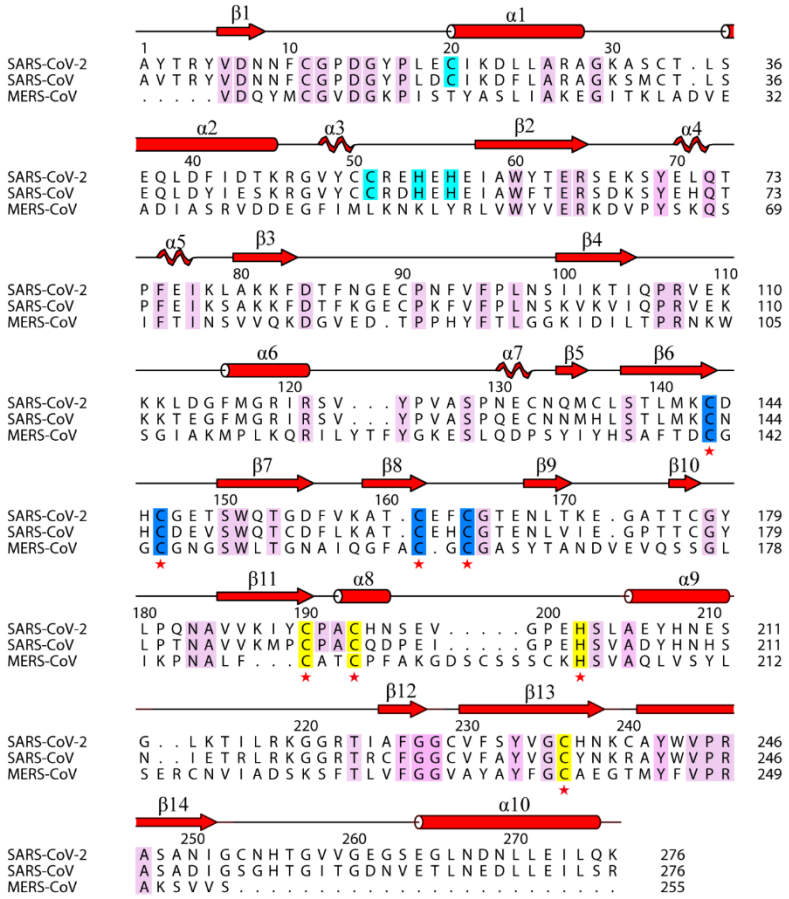

Fig. S1. Structure-based sequence alignment of nsp2$_{1\text{-}276}$ between SARS-CoV-2, SARS-CoV, and MERS-CoV. Secondary structural elements of the SARS-CoV-2 nsp2$_{1\text{-}276}$ structure were calculated using DSSP. Cylinders, waved lines and arrows represent α-helices, 3_{10} helices, and β-sheets, respectively. The residues coordinating the three zinc ions are shown as cyan, blue, and yellow, respectively, and red stars underneath show the conserved residues. Invariable residues between SARS-CoV-2, SARS-CoV, and MERS-CoV-2 are colored pink. According to the sequence conservation, the alignment was generated by ClustalW (Larkin *et al.* 2007) with manual adjustments of the MERS-CoV to make the residues coordinating the last two zinc ions align. This figure was made by the program ALINE (Bond and Schüttelkopf 2009). The sequences used are SARS-COV-2 (GenBank accession: QRW63624.1), SARS-CoV (ACZ72252.1), and MERS-CoV (ATQ39389.1).

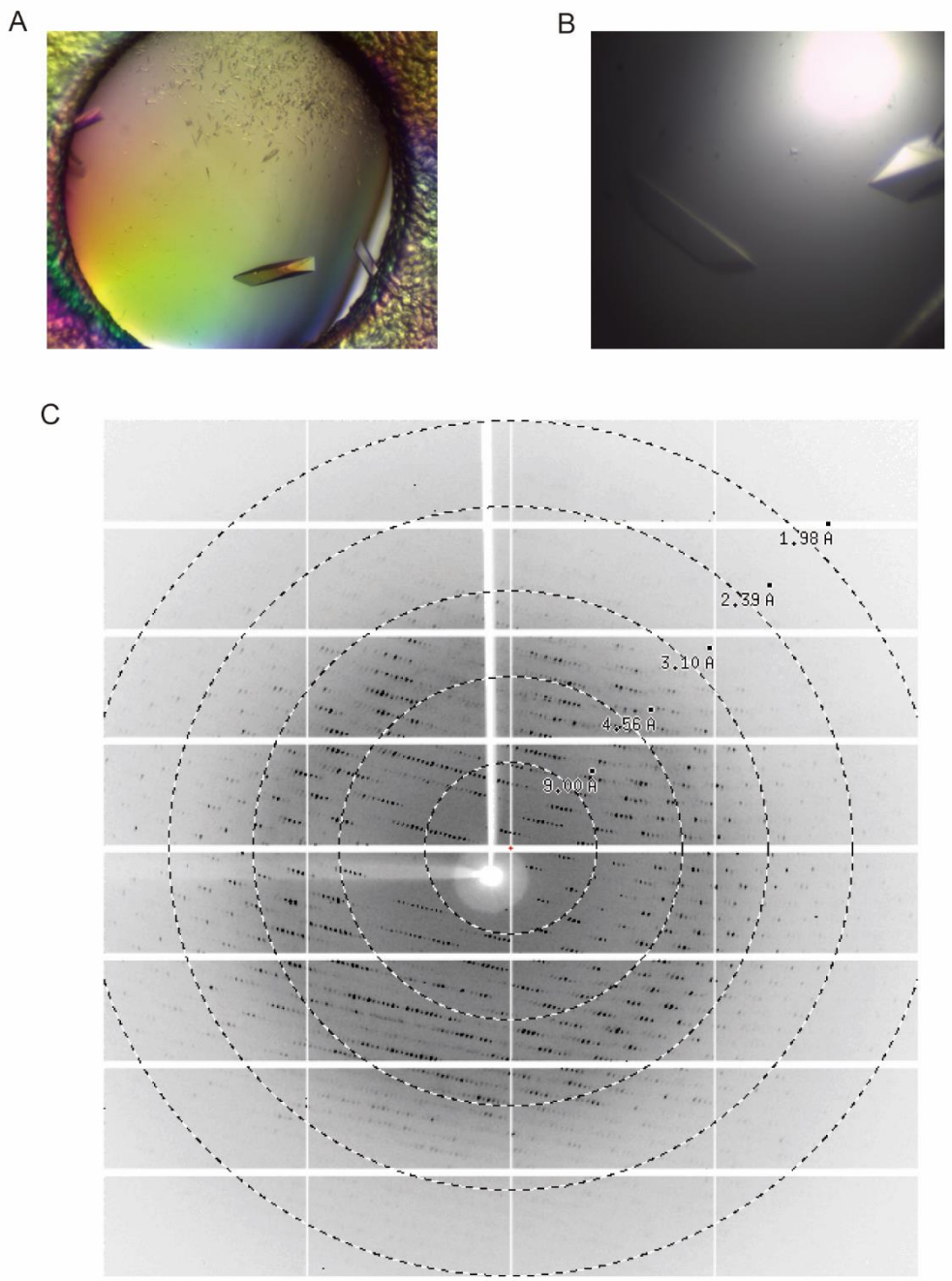

Fig. S2. Crystal optimization of nsp2$_{1-276}$. **A** Crystals grown by using the sitting-drop vapor diffusion method. **B** Optimized crystals by using the hanging-drop vapour-diffusion method. **C** X-ray diffraction image of nsp2$_{1-276}$.

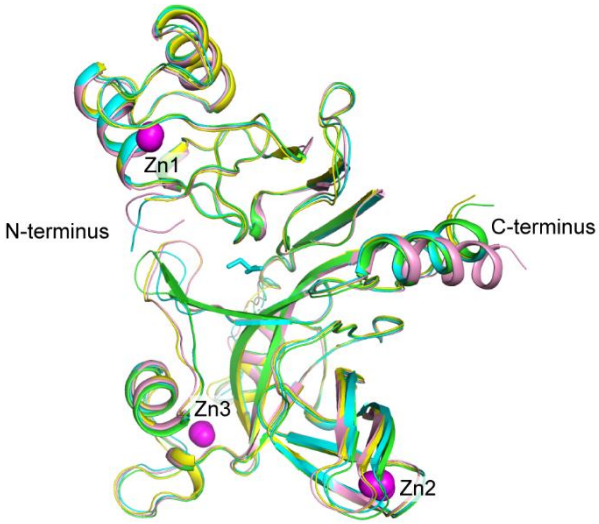

Fig. S3 Superposition of nsp2$_{1\text{-}276}$ A, B, C, D four chains. Four chains are shown in pink, yellow-orange, cyan, and green, respectively, and the three zinc atoms are shown as magenta.

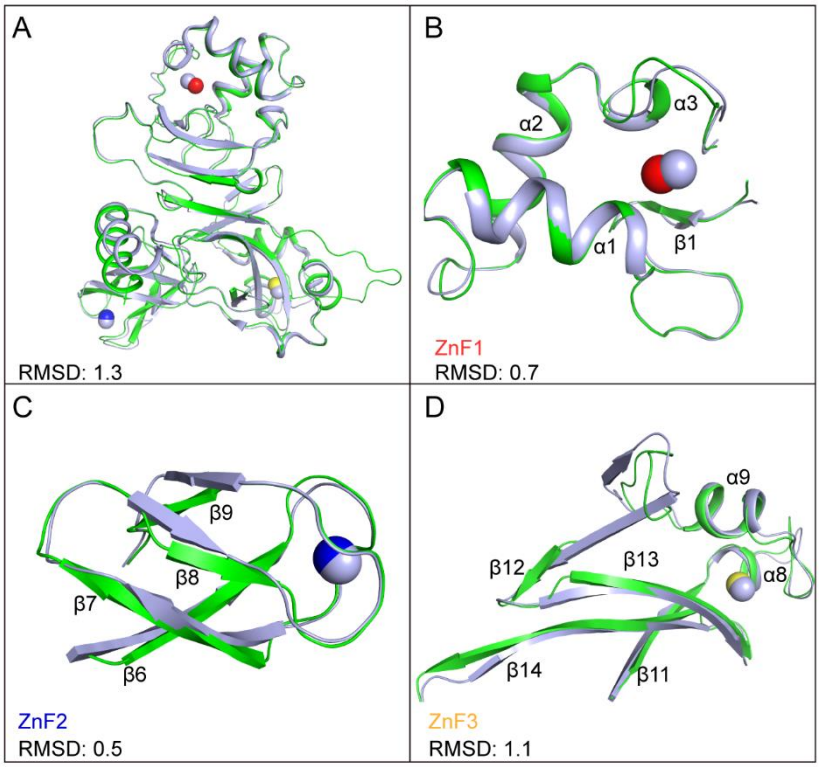

Fig. S4 Comparison of the Cryo-EM structure and the high resolution X-ray structure of nsp2$_{1\text{-}276}$. **A** Superposition of the Cryo-EM structure (PDB: 7MSW) (light-blue) and the overall high resolution X-ray structure of A chain of nsp2$_{1\text{-}276}$ (green) with RMSD of 1.3. Superposition of ZnF1 (**B**, Zn1, red), ZnF2 (**C**, Zn2, blue), and ZnF3 (**D**, Zn3, yellow) of the X-ray structure (green) and the Cryo-EM structure (light-blue) with RMSD of 0.7, 0.5, and 1.1, respectively.

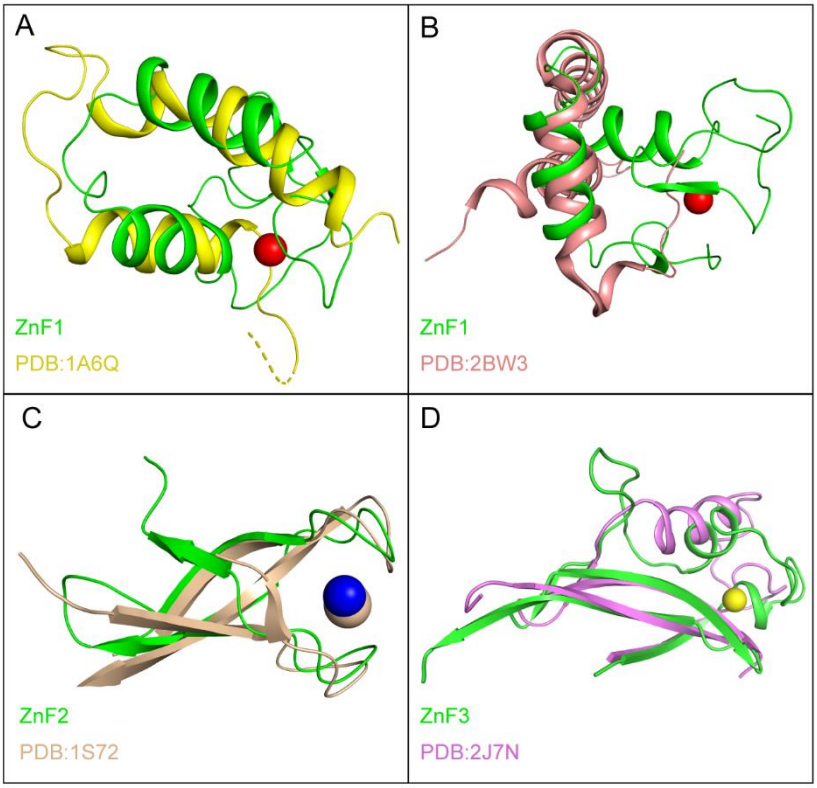

Fig. S5 Structural comparison of Zinc fingers. **A** Superposition of ZnF1 (green) and protein serine/threonine phosphatase 2C (PDB: 1A6Q) (yellow) with RMSD of 2.6 Å. Zn1, red (Das *et al.* 1996). **B** Superposition of ZnF1 and eukaryotic DNA transposase (PDB: 2BW3) (deep-salmon) (Hickman *et al.* 2005) with RMSD of 3.0 Å. **C** Superposition of ZnF2 (green) and 50S ribosomal protein L44E (PDB: 1S72) (wheat) (Klein *et al.* 2004) with RMSD of 1.8 Å. Zn2, blue. **D** Superposition of ZnF3 (green) and RNAi polymerase from *Neurospora crassa* (PDB: 2J7N) (violet) (Salgado *et al.* 2006) with RMSD of 2.4 Å. Zn3, yellow.

Table S1. SAXS data collection and analysis.

Parameters	**nsp2$_{1-276}$**
Data collection	
Instrument	SSRF BL19U2
Wavelength (Å)	1.003
Exposure time (s)	1.0
Concentration (mg/mL)	5.0
Temperature (K)	283
Structural parameters	
I(0) (from *P*(*r*))	68.2
R_g (Å) (from *P*(*r*))	23.2
I(0) (from Guinier)	70.4
R_g (Å) (from Guinier)	24.3
D_{max} (Å)	65
Porod volume V_p (Å^3)	52706.0
Correlation volume V_c (Å^2)	68049.0
Molecular mass	
Mass (kDa)[1]	30.8
Mass (kDa)[2]	30.0
Mass (kDa)[3]	25.6
Data processing	
Data reduction and processing	BioXTAS-RAW (Nielsen *et al.* 2009)
Validation	FoXS (Schneidman-Duhovny *et al.* 2013)
χ^2	4.69
c1, c2	1.04, 2.01

Table S2. List of primers for nsp2

Primer name	Sequence 5' → 3'
nsp2 *Eco*R I 5'	CTAATTATTCGAAACGAGGAATTCATGGCGTACACCCG TTATGTGGACAA
nsp2 *Kpn* I 3'	CTGGAAGTACAGGTTTTCGGTACCGCCACCCTTCAGG GTAAAGGTGTT
$nsp2_{1-276}$ *Bam*H I 5'	GCGGATCCGCGTACACCCGTTATGTGGACAA
$nsp2_{1-276}$ *Xho* I 3'	GCCTCGAGTTTTTGCAGAATCTCCAGCAGGTTGT
$nsp2_{1-276}$ K111A/K112A/K113A 5'	GTTGAGGCGGCAGCGCTGGATGGTTTTATGGGCCGTAT CCGTAGCGTGTAC
$nsp2_{1-276}$ K111A/K112A/K113A 3'	ATCCAGCGCTGCCGCCTCAACACGCGGTTGAATGGTT TTAATGATGCTGTTCAGC

References

Bond CS, Schüttelkopf AW (2009) ALINE: a WYSIWYG protein-sequence alignment editor for publication-quality alignments. Acta crystallographica Section D, Biological crystallography 65:510-512

Das AK, Helps NR, Cohen PT, Barford D (1996) Crystal structure of the protein serine/threonine phosphatase 2C at 2.0 A resolution. The EMBO journal 15:6798-6809

Hickman AB, Perez ZN, Zhou L, Musingarimi P, Ghirlando R, Hinshaw JE, Craig NL, Dyda F (2005) Molecular architecture of a eukaryotic DNA transposase. Nature structural & molecular biology 12:715-721

Klein DJ, Moore PB, Steitz TA (2004) The roles of ribosomal proteins in the structure assembly, and evolution of the large ribosomal subunit. J Mol Biol 340:141-177

Larkin MA, Blackshields G, Brown NP, Chenna R, McGettigan PA, McWilliam H, Valentin F, Wallace IM, Wilm A, Lopez R, Thompson JD, Gibson TJ, Higgins DG (2007) Clustal W and Clustal X version 2.0. Bioinformatics 23:2947-2948

Nielsen SS, Toft KN, Snakenborg D, Jeppesen MG, Jacobsen JK, Vestergaard B, Kutter JP, Arleth L (2009) BioXTAS RAW, a software program for high-throughput automated small-angle X-ray scattering data reduction and preliminary analysis. J Appl Crystallogr 42:959-964

Salgado PS, Koivunen MR, Makeyev EV, Bamford DH, Stuart DI, Grimes JM (2006) The structure of an RNAi polymerase links RNA silencing and transcription. PLoS biology 4:e434

Schneidman-Duhovny D, Hammel M, Tainer JA, Sali A (2013) Accurate SAXS profile computation and its assessment by contrast variation experiments. Biophysical journal 105:962-974